

# Summary

Because of climate change we observe a general advance of phenology in various species. Environmental fluctuations are also known to have great consequences on adaptation dynamics. Quantitative genetics models have been developed to predict those dynamics, focusing on quantitative traits with optimal values. None has investigated yet the impact of climate change with fluctuations on long-lived species such as tree. We model a stage-structured tree population in two stages: mature and immature individuals, each class having an optimal bud-burst value influencing their fitness components. We then vary optima with and without fluctuations. Fluctuations seem to decrease survival in our population, but as we focused on long-lived species there seem to be a buffer effect of our classes: they do not react very much to fluctuations. From PHENOFIT simulations we estimated a variation of optimal bud-burst date for fecundity of -0.15 day per year during the next century, we also showed a increase frequency of extreme events where all fecundities are equal to 0. However, our model does not take into account phenotypic plasticity which may decreases the observed genetic evolution.

## Introduction

Scientific consensus has been reached for several years about the rapid environmental change we are experiencing, a rise of more than 0.8°C in the 1901-2012 period (Stocker et al., 2013). But, the high interannual variability makes temperature fluctuating around the increasing trend.

The increase of temperature caused several organisms to advance in their phenology, i.e. the timing of various seasons. There have been evidences of trend to precocity in plants in their flowering time and bud-burst date (Alberto et al., 2011; Gienapp et al., 2013).

Models generally take into account a single trait with a single optimal value maximizing the fitness of an individual (Lande, 1982). To mimic variable environments they either vary the optimum in a linear fashion or randomly fluctuate it around a given mean (Lande and Shannon, 1996).

As long-lived species trees experience selection differently from annual plants, they buffer selection across several years, because of their particular stage structure: seedlings and grown trees do not experience the same selection pressures (Lande, 1982; Coulson and Tuljapurkar, 2008; Barfield et al., 2011; Engen et al., 2011).

Here we focused on the effect of fluctuations on a stage-structured tree population, with bud-burst date as the observed trait, and two different optima one from each stage. We used a previously developed demographic and quantitative genetics models (see ), and implemented environmental fluctuations. Using PHENOFIT's simulations we estimated those fluctuations in the wild.

## Materials and Methods

### Population model

We used a previously developed model with stage-structure (Sandell 2014, master's thesis). We considered a population of trees split in two classes, immature (I) and mature (M). only mature individuals reproduce. Each year, an immature individual can survive with a probability  $s_I$ , mature and reproduce with a probability of  $m$ . At the same time, a mature individual has a probability  $s_M$  to survive. First-time reproducers, i.e. immature that became mature and reproduce the same year, have a fecundity of  $f_1$ , while experienced reproducers, those who already reproduced at least once, have a fecundity of  $f_2$ . Produced seeds have a probability  $s_0$  to survive and join the pool of immature trees. The standard parameters set is given in (Table 1). The population census is just before reproduction. The population

dynamics can be predicted using the following matrix (Caswell, 2001):

$$A = \begin{pmatrix} a_{II} & a_{IM} \\ a_{MI} & a_{MM} \end{pmatrix} = \begin{pmatrix} s_0 m f_1 + s_I(1 - m) & s_0 f_2 \\ s_M m & s_M \end{pmatrix} \quad (1)$$

, where  $a_{ij}$ , the transition rate, describes the contribution of stage  $j$  individuals to stage  $i$  the next year. With given initial conditions we can compute the number of individuals in the two stages by iterating matrix multiplication by  $A$ .

I implemented density-dependence in this model, so that the population would not continuously increase (see Figure 1). I assumed seed germination and survival parameter  $s_0$  declined with increasing density of mature and immature competitors using a Beverton-Holt function (Caswell, 2001):

$$s_0 = \frac{s_{0,max}}{1 + k_I N_I + k_M N_M} \quad (2)$$

with  $k_I$  and  $k_M$  the weights of immature ( $N_I$ ) and mature ( $N_M$ ) population respectively.  $s_{0,max}$  is the maximum achievable  $s_0$ .

## Phenotype and life-history traits

We model the evolution of a phenotypic trait, e.g. the date at which first leafs appear on a tree,  $z$  the bud-burst date. In our model, an individual is born with a given phenotype and keeps it throughout its life.

Too early bud-burst can compromise the survival of young immature trees and the fecundity of mature trees because of the risk of frost. Too late bud-burst also affects the same traits because the bad season arrives before enough photosynthetates have been accumulated to guarantee survival of young trees and maturation of fruits. We assume that the survival of large mature trees is less sensitive to variation of phenology. We therefore supposed that for each individual -  $s_I$  immature survival,  $f_1$  first reproducers fecundity and  $f_2$  experienced reproducers - (see Equation 1) to be Gaussian function of phenotype  $z$ . Thus, bud-burst date directly influence their values. They are expressed as follow:

$$\begin{cases} s_I(z) = s_I(\theta_s) \exp\left(-\frac{(z - \theta_s)^2}{2\omega_s}\right) \\ f_1(z) = f_1(\theta_f) \exp\left(-\frac{(z - \theta_f)^2}{2\omega_f}\right) \\ f_2(z) = f_2(\theta_f) \exp\left(-\frac{(z - \theta_f)^2}{2\omega_f}\right) \end{cases} \quad (3)$$

,  $\theta_s$  is the optimal bud-burst date for survival, i.e. phenotype where  $s_I$  is at its maximum  $s_I(\theta_s)$ ;  $\omega_s$  is the width of the Gaussian function, its inversely related to selection intensity: with small  $\omega_s$  values, only a restricted range of bud-burst dates would have important survival rates.  $f_1$  and  $f_2$  have similar expressions, but the optimal bud-burst date  $\theta_f$  is different from  $\theta_s$ ,  $f_1$  and  $f_2$  only differ by their maximum values  $f_i(\theta_f)$ , with  $f_1$  lower than  $f_2$  (see Table 1 to have standard parameters values).

The optimal trait values  $\theta_s$  and  $\theta_f$  can differ between stages and life-history components, but trait value does not change along the life of an individual, then there is a trade-off between the two fitness components fecundity and immature survival. The evolution of the trait then affects the population dynamics through the life-history of the individuals in the population.

If we want to compute mean transition rate  $\overline{a_{ij}}$ , we need to average  $s_I$ ,  $f_1$  and  $f_2$  (ex:  $\overline{a_{IM}} = s_0 \overline{f_2}$ ):

$$E[s_I] = \overline{s_I} = \int p_I(z) s_I(z) dz \quad (4)$$

, with  $p_I(z)$  the distribution of  $z$  in the immature stage. We suppose  $p_I$  has a Gaussian distribution with mean  $\bar{z}_I$  and width  $P_I$  the phenotypic variance in the immature stage (Lande, 1982). We end with the following expression for  $\bar{s}_I$ :

$$\bar{s}_I(\bar{z}_I) = s_I(\theta_s) \sqrt{\frac{\omega_s}{\omega_s + P_I}} \exp\left(-\frac{(\bar{z}_I - \theta_s)^2}{2(\omega_s + P_I)}\right) \quad (5)$$

We obtain similar expressions for  $\bar{f}_1$  and  $\bar{f}_2$ .

## Iterations at each time step

Assuming the phenotype has a Gaussian distribution, the mean genotypic value of matures and immatures at the next time step is given by (Barfield et al. 2011 Eq.5, applied to the current models) :

$$\bar{g}_I' = (c_{IM}\bar{g}_M + c_{II}\bar{g}_I) + (c_{IM}G_M\beta_{a_{IM}} + c_{II}G_I\beta_{a_{II}}) \quad (6a)$$

$$\bar{g}_M' = (c_{MI}\bar{g}_I + c_{MM}\bar{g}_M) + (c_{MI}G_I\beta_{a_{MI}} + c_{MM}G_M\beta_{a_{MM}}) \quad (6b)$$

with  $c_{ij} = \frac{n_j \bar{a}_{ij}}{n'_i}$ , the contribution of stage  $j$  individuals to next years pool of stage  $i$  individuals, as a fraction of  $i$  individuals at the next time step  $n'_i$ ; and  $\beta_{a_{ij}}$  the selection gradient as  $\beta_{a_{ij}} = \frac{\partial \ln \bar{a}_{ij}}{\partial \bar{z}}$  (Barfield et al., 2011). The selection gradient represents the force of directional selection, and together with the genetic variance for the trait ( $G$ ), is used to predict the change in mean phenotype due to the response to selection (Lande, 1982).

The first term is a weighted average of mean genotypes contributing to this stage; while the second shows the effect of selection.

To have the formal expressions of  $\beta_{a_{ij}}$  we need to compute the selection gradients on life-history components:

$$\begin{aligned} \beta_{\bar{s}_I} &= \frac{\partial \ln \bar{s}_I}{\partial \bar{z}_I} = \frac{\theta_s - \bar{z}_I}{\omega_s + P_I} \\ \beta_{\bar{f}_1} &= \frac{\partial \ln \bar{f}_1}{\partial \bar{z}_I} = \frac{\theta_f - \bar{z}_I}{\omega_f + P_I} \\ \beta_{\bar{f}_2} &= \frac{\partial \ln \bar{f}_2}{\partial \bar{z}_M} = \frac{\theta_f - \bar{z}_M}{\omega_f + P_M} \end{aligned} \quad (7)$$

Because we have for example  $\bar{a}_{II} = s_0 m \bar{f}_1 + \bar{s}_I (1 - m)$  we get the selection gradient:

$$\beta_{a_{II}} = \frac{s_0 m \bar{f}_1 \beta_{\bar{f}_1} + \bar{s}_I \beta_{\bar{s}_I} (1 - m)}{\bar{a}_{II}} \quad (8)$$

We have a similar recursion for phenotypes (Barfield et al., 2011). We need to distinguish direct transitions of individuals from one stage to the other  $\bar{t}_{ij}$  and events leading to new individuals  $\bar{f}_{ij}$  (note  $\bar{a}_{ij} = \bar{t}_{ij} + \bar{f}_{ij}$ ), because in the first case the phenotype remain unchanged while in the second only the genotype is inherited:

$$\bar{z}_I' = c_{II}^t(\bar{z}_I + P_I \beta_{t_{II}}) + c_{II}^f(\bar{g}_I + G_I \beta_{f_{II}}) + c_{IM}^f(\bar{g}_M + G_M \beta_{f_{IM}}) \quad (9a)$$

$$\bar{z}_M' = c_{MI}^t(\bar{z}_I + P_I + \beta_{t_{MI}}) + c_{MM}^t(\bar{z}_M + P_M + \beta_{t_{MM}}) \quad (9b)$$

, with  $\beta_{t_{ij}}$  the gradient of selection defined as above in Equation 6a, i.e.  $\beta_{t_{ij}} = \frac{\partial \ln \bar{t}_{ij}}{\partial \bar{z}}$ ;  $c_{ij}^f = \frac{n_j \bar{f}_{ij}}{n'_i}$  the contribution by direct transition of stage  $j$  to stage  $i$  and  $c_{ij}^f = \frac{n_j \bar{f}_{ij}}{n'_i}$  the contribution by birth.

## Approximation under weak selection

Under weak selection, the mean phenotype at equilibrium in the population  $\bar{z}$  follows in a constant environment (Engen et al., 2011):

$$\bar{z}_{eq} = \frac{\gamma_f \theta_f + \gamma_s \theta_s}{\gamma_f + \gamma_s} \quad (10)$$

, with,

$$\gamma_f = \frac{v_I u_I s_0 m \bar{f}_1}{\lambda(P_I + \omega_f)} + \frac{v_I u_M \frac{G_M}{G_I} s_0 \bar{f}_2}{\lambda(P_M + \omega_f)} \quad (11a)$$

and

$$\gamma_s = \frac{v_I u_I \bar{s}_I (1 - m)}{\lambda(P_I + \omega_s)} \quad (11b)$$

$\gamma_f$  and  $\gamma_s$  represent the respective weight of each of the optimum in the trade-off between  $\theta_f$  and  $\theta_s$  for  $\bar{z}_{eq}$ . Indeed, if  $\theta_f = \theta_s$  then  $\bar{z}_{eq} = \theta_f = \theta_s$ . But if  $\theta_f \neq \theta_s$ , then the position of the mean phenotype depends on  $\gamma_f$  and  $\gamma_s$ .

## Fluctuating optimums

I introduced environmental fluctuations in the model through the optima:

$$\begin{cases} \theta_f(t) = \bar{\theta}_f + \alpha_f \xi_f \\ \theta_s(t) = \bar{\theta}_s + \alpha_s \xi_s \end{cases} \quad (12)$$

$\alpha_i$  is the sensitivity of  $\theta_i$  to noise  $\xi_i$ .  $\xi_f$  and  $\xi_s$  are noise vectors drawn at each time step from a bi-variate normal distribution with respectively  $\sigma_f^2$  and  $\sigma_s^2$  variances and correlation  $\rho_N$ .

Under varying environment we get another approximation under weak selection from (Engen et al., 2011) describing the change of mean phenotype:

$$\Delta \bar{z}(t) = -G_I \gamma (\bar{z}(t) - \theta_v(t)) \quad (13)$$

, with

$$\gamma = \gamma_f + \gamma_s \quad (14a)$$

$$\theta_v(t) = \bar{z}_{eq} + \xi_v \quad (14b)$$

$$\xi_v = \frac{\alpha_f \xi_f + \alpha_s \xi_s}{\alpha_f + \alpha_s} \quad (14c)$$

We see that the change in the mean phenotype depends on the sensitivity of the optima  $\alpha_i$  as well as on the magnitude of the variations.

## Trend in change

To model climate-change, and especially the trend of increasing temperature with time, we included a trend in the variation of the optima:

$$\begin{cases} \theta_i(t) = \bar{\theta}_i + \alpha_i \epsilon(t) \\ \epsilon(t) = kt + \xi_i \end{cases} \quad (15)$$

With  $k$  having a negative value, the optima tend to decrease with time.

## PHENOFIT data

PHENOFIT is a phenology model including several sub-models, from environmental and phenological data it simulates the survival and reproduction of an average tree to predict its range (Morin et al., 2008).

We used output from PHENOFIT (simulations performed by A. Duputié) from 1950 to 2100 for the sessile oak (*Quercus petraea*) about predicted bud burst date and predicted fitnesses in 6 localities (see Figure 4). We had fitness and fecundity predictions for phenotypes around the modeled date (a range of 21 days). From these data we predicted the optima fluctuations. Considering fecundity  $f$  as a Gaussian function around this date with the same form as  $f_1$  in Equation 5:

$$\beta = \frac{\partial \ln f}{\partial \bar{z}} = \frac{\theta_f - \bar{z}}{\omega_f + \sigma_z^2} \quad (16)$$

Using (Lande and Arnold, 1983), with  $z$  Gaussian,  $p(z)$  the distribution of  $z$  in the population,  $f(z)$  the fitness associated with  $z$  and  $\bar{f}$  the mean fitness in the population, we computed selection gradients from PHENOFIT simulation outputs as:

$$\beta = \frac{\text{cov}(z, \frac{f(z)}{\bar{z}})}{\sigma_z^2} \quad (17)$$

From (16) and (17) we can express  $\theta_f$ :

$$\theta_f = \frac{\text{cov}(z, \frac{f(z)}{\bar{z}})}{\sigma_z^2}(\omega_f + \sigma_z^2) + \bar{z} \quad (18)$$

In our estimations we considered  $p(z)$  to be Gaussian around the modeled date by PHENOFIT, with a variance of  $P_I = 40$  as in our analytic model. We normalized this distribution so that all dates in the population would be in the 42 days interval around the modeled date.

## Trend analyses

All statistical analyses were made using R (R Core Team, 2014), graphics were drawn using ggplot2 (Wickham, 2009), data were handled using dplyr (Wickham and Francois, 2014).

To estimate the trend of the  $\theta_f$  variations, we considered a trend model with three components: a general decreasing linear trend, a white noise component with a constant variance and a more dramatic noise leading to "catastrophic" events, with low  $\theta_f$  values.

The regular noise and the trend were estimated excluding those catastrophic events, we kept only value of  $\theta_f$  over 60, which is the lower bound of the realizable range of bud burst date of oak trees. Then we performed a linear regression between values of  $\theta_f$  and time, giving us an estimation of  $k$  from Equation 15. Analyzing the residuals gives us the variance of  $\alpha_f \xi_f$  from the same equation.

## Results

### Constant environment and density-dependence

We used the previously developed model in (Sandell 2014) and simulated (see Figure 1) a tree population for 150 years in a constant environment, with and without density-dependence on  $s_0$ , assess the effects of a more realistic demography.

As expected, density-dependence allows regulating the population (Figure 1 right panel), as the number of mature and immature individuals seem to converge respectively to 18000 and 10000 individuals, while without density-dependence the population is exponentially growing.

Parameter	Notation	Value
<b>Life Cycle</b>		
Optimal phenotype for fecundity	$\theta_f$	100
Optimal phenotype for immature survival	$\theta_s$	130
Fecundity function width	$\omega_f$	400
Survival function width	$\omega_s$	400
Heritability	$h^2$	0.5
Phenotypic variance of immatures	$P_I$	40
Phenotypic variance of matures	$P_M$	40
Genotypic variance of immatures	$G_I = P_I \times h^2$	20
Genotypic variance of matures	$G_M$	20
Survival of immature at phenotypic optimum	$\overline{s_I}(\bar{z} = \theta_s)$	0.8
Fecundity of first time reproducers at optimum	$\overline{f_1}(\bar{z} = \theta_f)$	100
Fecundity of experienced reproducers at optimum	$\overline{f_2}(\bar{z} = \theta_f)$	200
Maturation rate of immature	$m$	0.02
Combined survival and germination rate of seed	$s_0$	0.03
Survival of mature stage	$s_M$	0.99
<b>Density-dependence</b>		
Maximum $s_0$ in density-dependence function	$s_{0,max}$	0.12
Decreasing factor due to immatures	$k_I$	0.001
Decreasing factor due to matures	$k_M$	0.005
<b>Fluctuations</b>		
Sensitivity of optimum for fecundity to fluctuation	$\alpha_f$	5
Sensitivity of optimum for survival to fluctuation	$\alpha_s$	5
Noise variance for fecundity	$\sigma_{\xi_f}^2$	3.725
Noise variance for survival	$\sigma_{\xi_s}^2$	3.725
Correlation between noises	$\rho_N$	0.5
Trend coefficient	$k$	-0.15

**Table 1:** Standard parameter set

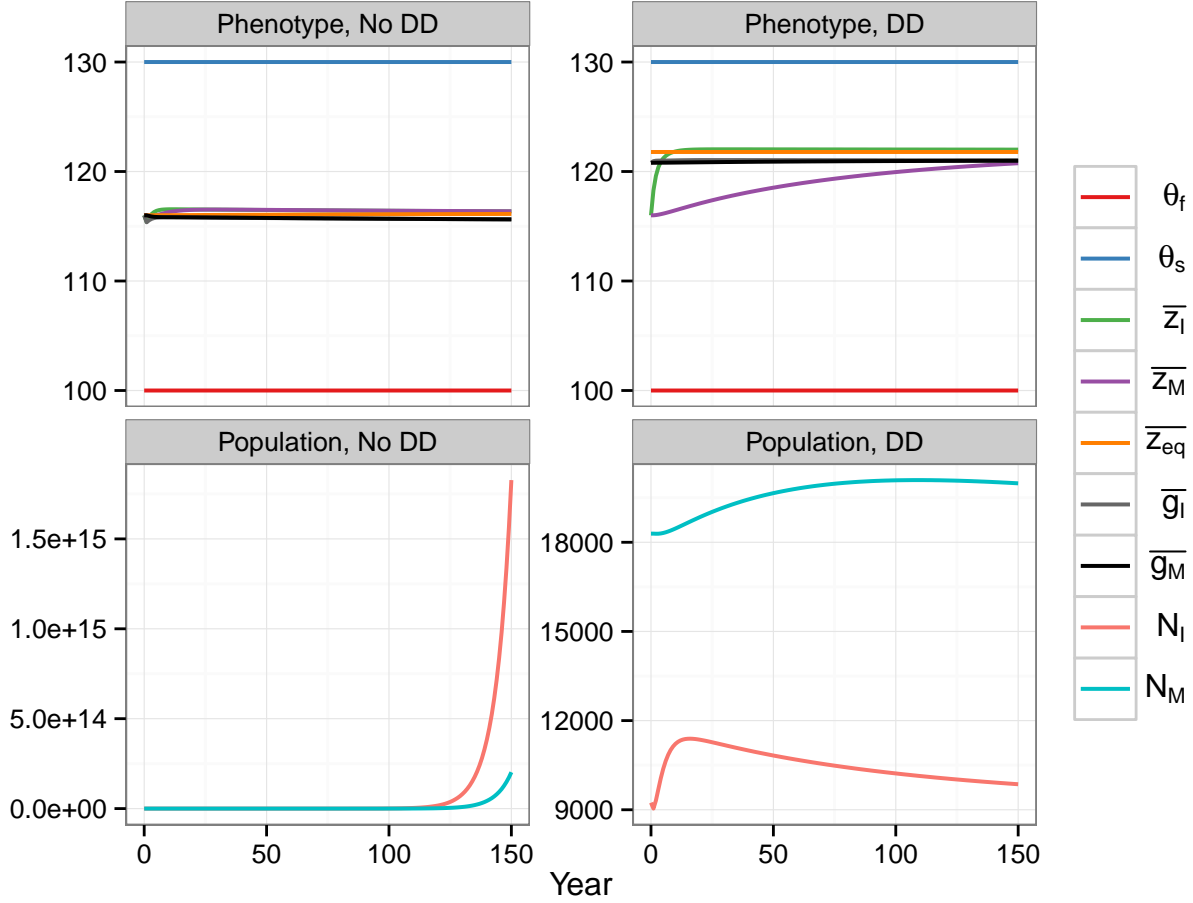


**Figure 1: Effect of density-dependence on phenotypes and populations.** **Top:** Phenotype variations in population ( $\bar{z}_I$ ,  $\bar{z}_M$ , starting from  $z = 116$ ) with their corresponding genotypic values ( $\bar{g}_I$ ,  $\bar{g}_M$ ), and the approximation given by Equation 10; **Bottom:** Population, number of immature individuals ( $N_I$ , red), number of mature individuals ( $N_M$ , blue). Starting from Stable-Stage Distribution (SSD) in constant environment. **No DD** means we used the model without density-dependence, **DD** means we implemented density-dependence through  $s_0$  (see Equation 2). Here, bud-burst date is expressed in julian days (numbered days in the year, 1st of January being 1 in julian days).

Looking at the phenotype, we started from exactly the same starting point  $z = 116$  for phenotypic and genotypic values. Without density-dependence, the population quickly converge to the equilibrium phenotype ( $\bar{z}_{weak}$  given by the approximation in Equation 10),  $\bar{z}_{eq} = 116$  in this case. With density-dependence the equilibrium phenotype is shifted towards the survival optimum  $\theta_s$  ( $\bar{z}_{weak,dd} = 121.8$ ,  $\theta_s = 130$  while  $\theta_f = 100$ ). The lower seed survival  $s_0$  decreases  $\gamma_f$  (11a) changing the weights in (10), making it more interesting to favor the survival of already established immature trees than the production of many propagules with very little survival prospect.

The genotypic values,  $\bar{g}_I$  and  $\bar{g}_M$  (respectively gray and black on Figure 1) are clearly distinct from the mean phenotype values.

The mean immature phenotype  $\bar{z}_I$  converge quicker than the mean mature phenotype  $\bar{z}_M$  to  $\bar{z}_{eq}$ . High mature trees survival in our simulations makes it long to replace them with a different genotype and phenotype. To make  $\bar{z}_M$  closer to  $\bar{z}_{eq}$ , immature individuals with a phenotype closer to  $\bar{z}_{eq}$  need to survive long enough to mature and outnumber initial mature individuals with phenotype further from  $\bar{z}_{eq}$ .

## Fluctuating optima

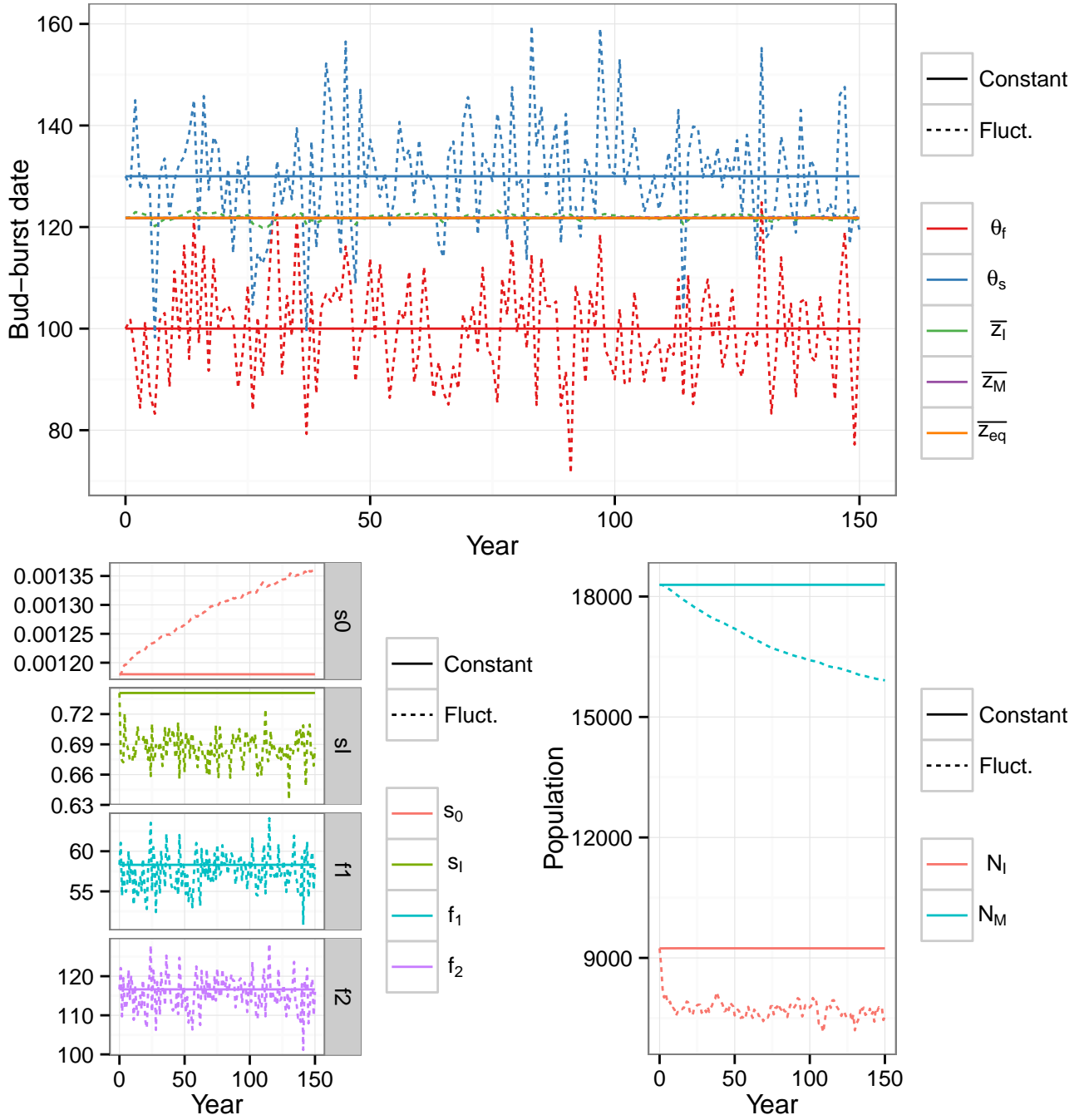


**Figure 2: Fluctuating optima against constant environment.** **Top:** comparison of phenotypes from simulations with constant or fluctuating optima,  $\bar{z}_{eq}$  is the approximation shown in Equation 10 results from single simulation. **Bottom: (Left)** life-history traits in constant or fluctuating environment, **(Right)** population in constant or fluctuating environment,  $N_I$  is the number of immature individuals and  $N_M$  the number of mature individuals, population started from the stable stage distribution. **Solid lines:** values in constant environment, **Dashed lines:** in fluctuating environment, results were averaged over 100 independent simulations.

To mimic a changing environment we made the optima fluctuate (Figure 2, dashed lines) and compared this model to the one in constant environment (solid lines).

The mean phenotype of the population does not change very much with the fluctuations, indeed,  $\bar{z}_M$  in constant and fluctuating environment are equal, and they are also equal to  $\bar{z}_{eq}$ , that is why they are indistinguishable on Figure 2.



Only  $\bar{z}_I$  fluctuates under varying environment, but the fluctuations have a very small variance compared to the ones of the optima. We found a strong correlation between  $\theta_s$  and  $\bar{z}_I$  across years ( $\rho_{\text{Pearson}} = 0.6997364$ ) than with  $\theta_f$ . It shows how immature individuals track the variations of the survival optimum and invest specifically more on this fitness component.

Because of the variations the phenotype lags away from the optimal value, decreasing the mean of  $s_I$  in fluctuating environment. The number of immature individuals  $N_I$  is thus lower under the fluctuating regime than decreasing the number of mature individuals  $N_M$ , this decline in density in turn increases  $s_0$ . The variation in  $\theta_s$  causes  $s_I$  to decrease, it reveals the cost of the fluctuations demographically: fluctuating regime causes variations in survival that may have dramatic effect on population.

However, those fluctuations do not seem to affect fecundities  $f_1$  and  $f_2$  in the same way (Figure 2 bottom left panel). As the mean optima move they get closer to population phenotype increasing fecundity, but the next time step they move further away from this phenotype and they decrease fecundity.

The asymmetry of responses between survival  $s_I$  and fecundities  $f_1$  and  $f_2$ , are explained by the specific trade-off occurring in our population. The mean phenotype in our simulations is closer to  $\theta_s$  than to  $\theta_f$ , there is a higher chance of  $\theta_s$  to be lower or much higher than the mean population phenotype, then there is for  $\theta_f$  to cross the mean population phenotype line.

As we had partially correlated noises in our population (see Table 1 to have standard parameters set), we vary correlations for noises between 0 and 1. The results were similar whatever the correlation coefficient. It seemed that the lower the correlation between noises, the higher were the demographic burden (results unshown). Uncorrelated environments decrease more the life-history traits than correlated environments.

## Trend in the environment

We implemented a decreasing trend in  $\theta_f$  with fluctuations (Figure 3) to mimic climate change. We simulated both a linear trend and a linear trend with fluctuations in optima variation (respectively solid and dashed lines in Figure 3).

The phenotype in the population decreases as the optima decrease, but much slower, whether with fluctuations or not. The mean phenotype in the immature stage  $\bar{z}_I$  seem to vary in the same fashion with and without fluctuations, while the mean phenotypes among mature individuals  $\bar{z}_M$  are almost indistinguishable in the two types of environments,  $\bar{z}_M$  under fluctuations (dashed line) is a little bit over  $\bar{z}_M$  without them (solid line). We implemented the approximation  $\bar{z}_e$  from (Engen et al., 2011), it seems to follow the variations in a similar fashion as the mean phenotype of the mature individuals.

The immature survival ( $s_I$ ) has an interesting behavior, it first increases, reaches a maximum, then decreases. The decreasing trend in optima variation causes at first the mean population phenotype to move closer to  $\theta_s$ , thus maximizing  $s_I$  values when it crosses  $\theta_s$  line, as soon as it moves beyond  $s_I$  starts to decrease again.

On the contrary  $f_1$  and  $f_2$  the mean population phenotype go further away from  $\theta_f$  with and without fluctuation.

After a certain number of years, population is lower in environments with trends than in constant ones, the effect is especially visible in the environments without fluctuations (Figure 2 & Figure 3 bottom right panel). However, fluctuations in constant environment seem to decrease more the number of immature individuals than the trend does in constant environment.

As expected, the decreasing trend in  $\theta_f$  creates a lag between the optima and the mean population values, because adaptation is slower than the rate of change. However, the population can still survive with such a rate if the difference between the optima and the means become constant. On a very long scale (2500 years) it is what happens in this case, the population maintains itself by changing its phenotype fast enough to track the optima variation (data not shown).

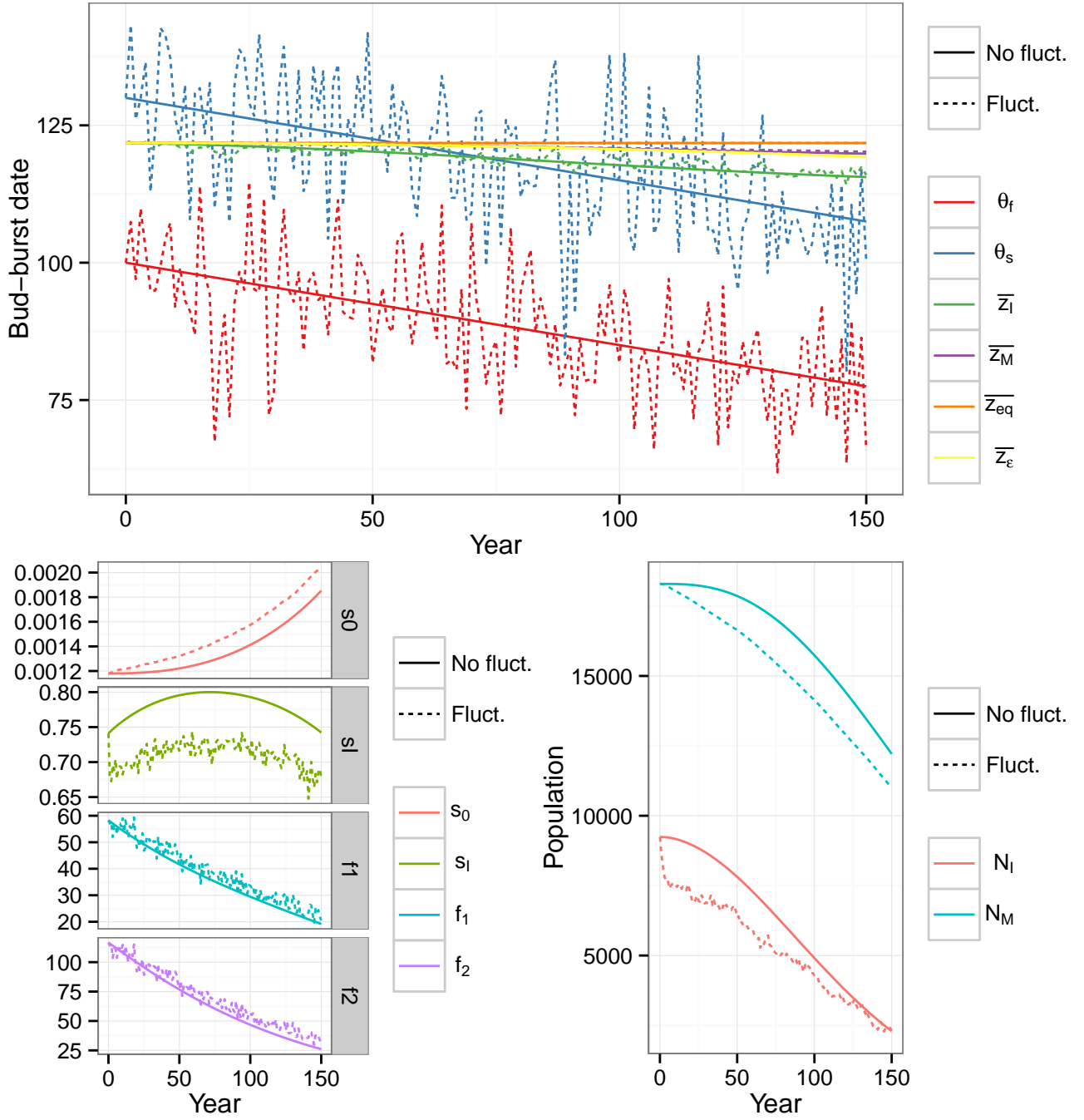


**Figure 3: Mixed influences of trend and fluctuations on the population.** **Top:** Phenotype evolution with and without fluctuations, results from a **single** simulation; **Bottom: (Left)** life-history traits evolution; **(Right)** demography. **Solid lines: (No fluct.)** linearly decreasing optima with time; **Dashed lines: With fluct.** fluctuating decreasing optima, results were averaged over 100 independent simulations.

## Estimation of the fluctuations

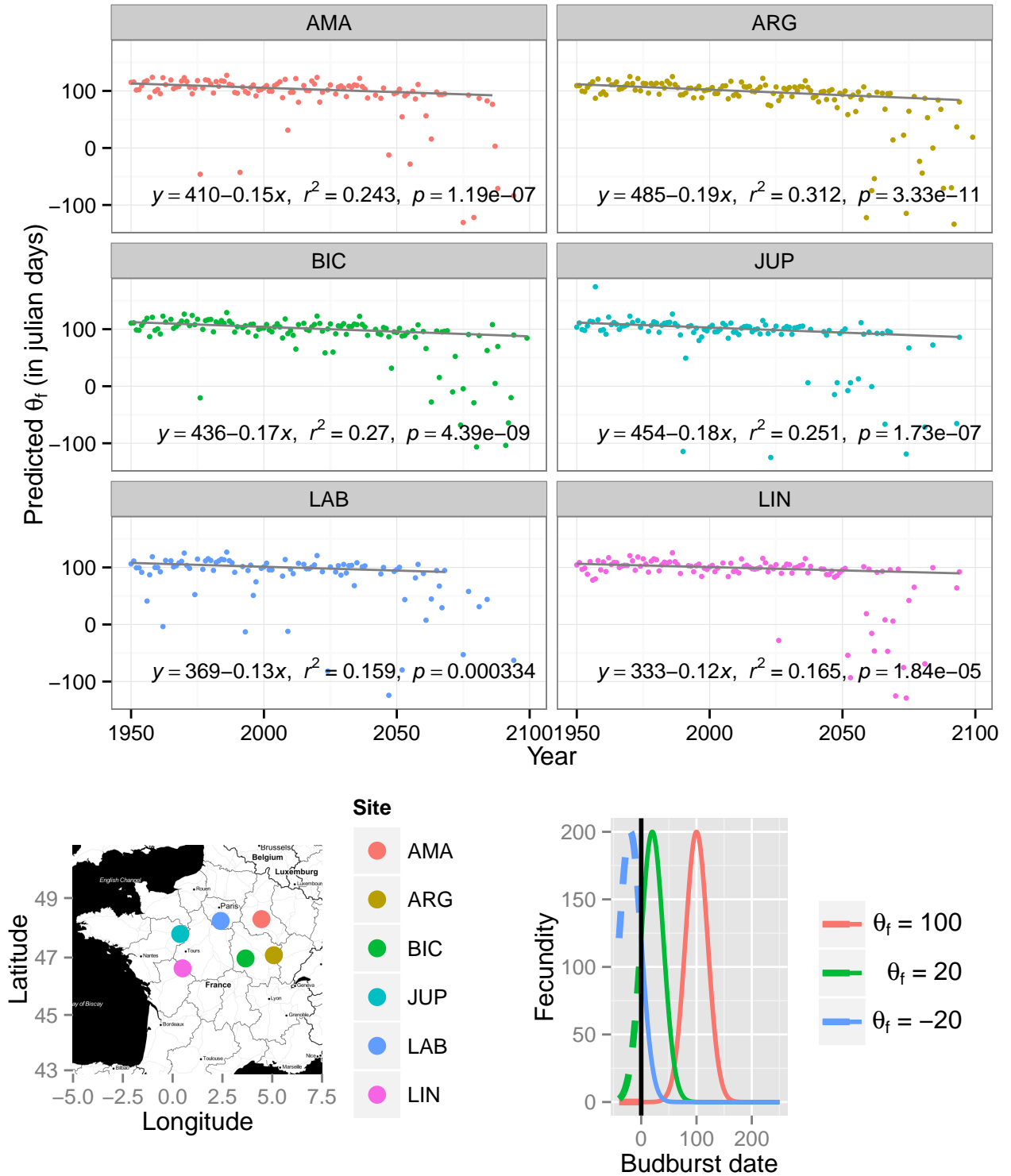


**Figure 4:**  $\theta_f$  estimations from PHENOFIT data. **Top:** estimations of  $\theta_f$  for each study site (see [Materials and Methods](#) for details), linear regression only for values  $>60$ . **Bottom: (Left)** map of the study sites; **(Right)** Theoretical fecundity functions with parameters from [Table 1](#) with values of  $\theta_f$  equals to 100, 20 and  $-20$ , solid lines indicate achievable phenotype, dashed lines show theoretical curves but unreachable phenotypes.

In 6 localities (map [Figure 4](#) bottom left) using PHENOFIT output, we computed  $\theta_f$  values at these locations (top 3 rows of [Figure 4](#)). For the 6 sites, predicted  $\theta_f$  decreases with time: earlier bud-burst

is favored as climate warms.

Over the general trend, we observe a small amplitude variation, corresponding to year to year change in  $\theta_f$  and some more episodic dramatic decreases in its values, sometimes reaching negative values (e.g. at BIC site in 1976). The frequency of these events increase with time as they become common after 2050 for all sites. Note that those events are biased towards the decrease of  $\theta_f$ , as there is no equivalent dramatic increases.

The negative values of  $\theta_f$  computed in [Figure 4](#), may seem striking as there is no such thing as a negative bud-burst date! It indicates strong directional selection to shorten bud-burst those years with very little sign of quadratic selection on that trait. As bottom right panel of [Figure 4](#) shows, we can have negative value of  $\theta_f$  and still have achievable phenotypes. If  $\theta_f$  is very negative for a given year (less than -100 in 2048 for LAB), it means there will be no reproduction this year (flat tail of blue curve, bottom right panel [Figure 4](#)).

We excluded those extreme events, taking all sites together, to estimate the trend in the variation of  $\theta_f$  (see [Materials and Methods](#)). Using linear regression on  $\theta_f$  with time, we found a rate of  $-0.15\text{day}\cdot\text{year}^{-1}$ , with normal residuals having a variance of  $105\text{day}^2$  (data not shown,  $R^2 = 0.2341$ ,  $p < 2\text{e-}16$ ,  $F = 186.7$  with 611 d.f.).

## Discussion

We modeled a stage-structured tree population using a quantitative genetics approach, with bud-burst date varying between two optima. We predicted phenotype evolution in the next 150 years. Using PHENOFIT simulation results we computed values for one of the optima. According to simulations, an increasing number of extreme events will happen in the next century where all fecundities will be equal to zero.

As expected in the literature, we found a decreasing trend in the variation of optima, i.e. a trend to precocity of phenology ([Aitken et al., 2008](#); [Ehrlén and Münzbergová, 2009](#)). Because of the general increase in temperature, organisms advance their phenology to track their original environment.

Genotypic ( $\bar{g}_i$ ) and phenotypic ( $\bar{z}_i$ ) values are different in our simulations (see [Figure 1](#)); because of both stage-structure and the two optima we use.

Density-dependence pushes the equilibrium phenotype  $\bar{z}_{eq}$  towards the survival optimum  $\theta_s$ , with higher intra-specific competition (due to [Equation 2](#)) it increases fitness to produce less seedlings and increase their survival than to produce more seeds with poor survival.

In constant environment with fluctuations, mean phenotypes in immature and mature stages do not show strong fluctuating pattern. Only the mean phenotype among immature individuals shows fluctuations, tracking closer the survival optimum  $\theta_s$  than the survival optimum  $\theta_f$ . The model consider long-lived species such as trees, on average it takes 40 years for an immature to become mature, and it can live several centuries after that.

Depending on the position of the mean phenotype in population, fluctuations may have a positive or a negative effect. If the mean phenotype is already near the optimal value, in our case near one of the optimum, the fluctuation of this optimum can only move it away from the mean phenotype—having a negative fitness impact; if the mean phenotype is far from an optimal value, then fluctuations have a higher chance to bring it closer to the mean phenotype value—having a positive impact on fitness. According to the position of the trade-off between optima fluctuations have positive or negative consequences on fitness, there is no general pattern understandable simply by observing fluctuations.

With trend ([Figure 3](#)), counter-intuitively, there is no difference of in adaptation speed with and without fluctuations. We could have expected an additional cost of fluctuations: if the population would have tracked fluctuations closely, then a increased noise variance would have decrease fitness dramatically, since it is not the case for reasons cited above, we see no cost of fluctuations when there is a general trend in the environment.

From the same case, we see the mean phenotype in immature individuals  $\bar{z}_I$  changes faster than the mean phenotype in mature individuals  $\bar{z}_M$ , there is a difference of adaptation speed between stages. The stage-structure of our population may explain the different behaviors among the two classes.

Our model was parametrized according to the sessile oak life-cycle (*Quercus petraea* spp.), using our simulations as prediction, with the estimated fluctuations and trend, the species does not go extinct in the next 150 years (Figure 3). Climate change has still dramatic demographic consequences, the population halving in less than 100 years. The sessile oak would be left more vulnerable demographically as it increases genetic drift and the potential force of dramatic events.

Those estimations and fluctuations do not include the extreme years when all fecundities are equal to zero, i.e. the selection gradient is zero, they affect adaptation dynamics. Modeling correctly the variations of optima values would lead to more realistic behavior, it could be done by drawing the optima from an almost gaussian distribution with a very long tail towards negative values.

Phenotypic plasticity should also be taken into account in a future model as it slows down genetic adaption. It has been shown to be an important component of adaptation to environmental changes (Aitken et al., 2008).

## Authors Contributions and Acknowledgments

M. Grenié did the analyses and simulations, based on L. Sandell's work. O. Ronce and LM. Chevin supervised the project. A. Duputié shared PHENOFIT outputs. I. Chuine advised the project about PHENOFIT outputs.

I would like to thank Ophélie Ronce for being an extremely patient supervisor, Luis-Miguel Chevin and Isabelle Chuine for the discussions we had about the project. I thank Guillaume Martin for being an awesome office-mate. Finally, I would like to thank the whole "Metapopulations" team at ISEM for their welcome.

## References

- Aitken, S. N., Yeaman, S., Holliday, J. A., Wang, T. and Curtis-McLane, S. (2008). Adaptation, migration or extirpation: climate change outcomes for tree populations. *Evolutionary Applications* 1, 95--111.
- Alberto, F., Bouffier, L., Louvet, J.-M., Lamy, J.-B., Delzon, S. and Kremer, A. (2011). Adaptive responses for seed and leaf phenology in natural populations of sessile oak along an altitudinal gradient. *Journal of Evolutionary Biology* 24, 1442--1454.
- Barfield, M., Holt, R. D. and Gomulkiewicz, R. (2011). Evolution in Stage-Structured Populations (2 versions). *The American Naturalist* 177, 397--409.
- Caswell, H. (2001). *Matrix population models : construction, analysis, and interpretation*. Sinauer Associates.
- Coulson, T. and Tuljapurkar, S. (2008). The Dynamics of a Quantitative Trait in an Age-structured Population Living in a Variable Environment. *Am Nat* 172, 599--612.
- Ehrlén, J. and Münzbergová, Z. (2009). Timing of Flowering: Opposed Selection on Different Fitness Components and Trait Covariation. *The American Naturalist* 173, 819--830.
- Engen, S., Lande, R. and Sæther, B.-E. (2011). Evolution of a Plastic Quantitative Trait in an Age-Structured Population in a Fluctuating Environment. *Evolution* 65, 2893--2906.

- Gienapp, P., Lof, M., Reed, T. E., McNamara, J., Verhulst, S. and Visser, M. E. (2013). Predicting demographically sustainable rates of adaptation: can great tit breeding time keep pace with climate change? *Phil. Trans. R. Soc. B* 368, 20120289.
- Lande, R. (1982). A Quantitative Genetic Theory of Life History Evolution. *Ecology* 63, 607--615.
- Lande, R. and Arnold, S. J. (1983). The Measurement of Selection on Correlated Characters. *Evolution* 37, 1210--1226.
- Lande, R. and Shannon, S. (1996). The Role of Genetic Variation in Adaptation and Population Persistence in a Changing Environment. *Evolution* 50, 434.
- Morin, X., Viner, D. and Chuine, I. (2008). Tree species range shifts at a continental scale: new predictive insights from a process-based model. *Journal of Ecology* 96, 784--794.
- R Core Team (2014). R: A Language and Environment for Statistical Computing. R Foundation for Statistical Computing Vienna, Austria.
- Stocker, T. F., Qin, D., Plattner, G. K., Tignor, M., Allen, S. K., Boschung, J., Nauels, A., Xia, Y., Bex, B. and Midgley, B. M. (2013). IPCC, 2013: climate change 2013: the physical science basis. Contribution of working group I to the fifth assessment report of the intergovernmental panel on climate change. .
- Wickham, H. (2009). *ggplot2: elegant graphics for data analysis*. Springer New York.
- Wickham, H. and Francois, R. (2014). *dplyr: A Grammar of Data Manipulation*. R package version 0.3.0.2.